**Proceedings of the ASME 2010 3rd Joint US-European Fluids Engineering Summer Meeting and 8th International Conference on Nanochannels, Microchannels, and Minichannels**
**FEDSM-ICNMM2010**
**August 1-5, 2010, Montreal, Canada**

# FEDSM-ICNMM2010-30281

## Formation Mechanism and Characteristics of Liquid Microlayer in Mini-gap Boiling System

**Yaohua Zhang**
Graduate school of Engineering,
Yokohama National University
Yokohama,Japan

**Yoshio Utaka**
Faculty of Engineering,
Yokohama National Univeristy
Yokohama,Japan

## ABSTRACT
Experiments were performed using the laser extinction method to directly measure the thickness of the liquid film between the bubbles and heating plates in a mini-gap formed by two parallel vertical quartz glass plates for the dielectric fluid HFE-7200 at gap sizes of 0.15, 0.3 and 0.5mm. High-speed movies were also taken to measure the velocity of bubble forefront simultaneously. It was confirmed that the microlayer thickness was determined by the gap size and velocity of bubble forefront. At the region of small Weber number, microlayer thickness of HFE-7200 was obviously thicker than that of water, toluene and ethanol at the same velocity and gap size for its small surface tension. Furthermore, by nondimensional analyzing of experimental data, the empirical correlation proposed in previous study which was based on water, toluene and ethanol is still reliable for HFE-7200.

## INTRODUCTION
Mini-gap type heat sinks are considered as one possible approach to satisfy the ever-increasing heat flux demand on cooling of electronic chips and the microelectronic devices. For practical application of the liquid cooling electronic equipment, dielectric fluid such as HFE7200 is often employed to avoid electric hazards. However, researches on the heat transfer and fluid flow characteristics concerning with dielectric fluids in mini-gap with flat parallel walls were comparatively rare. Phase-change heat transfer mechanisms and characteristics for the micro-scale boiling show distinct from macro-scale behavior. In mini-gap, bubbles nucleate and quickly grow to the channel size such that the elongated bubbles are formed and confined by the channel walls. It grows very fast in length with a dynamic tip defined as the forefront part of bubble where the curvature of interface between the bubble and liquid is obviously bigger than zero, and a microlayer is formed between the bubbles and inner heating plate walls simultaneously just behind the dynamic tip of bubble as shown in Fig.1. The bubble inside mini-gap is confined so much that the tip is just extremely small part of the bubble entire, whereas most part of it is surrounded by the microlayer that almost parallel with the heating plate. Also, as the fluid system becomes progressively smaller, the importance of surface tension increases. Moreover, the bulk liquid, superheated microlayers, and vapor bubbles in the mini-gap affect each other in complex ways. The transient evaporation of the microlayer elongated bubbles has been considered to be a major heat transfer mechanism.

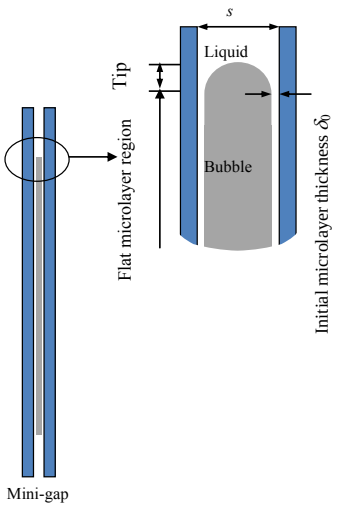


Fig.1 Schematic diagram of bubble in mini-gap

In a previous report on the present work [1] the thickness of microlayer that formed on a heating surface by vapor growth was measured by laser extinction with the testing liquids of

water, ethanol and toluene. It was found that the trend in the variation of microlayer thickness relative to the velocity of the bubble forefront could be divided into two regions. Furthermore, in order to clarify the basic formation mechanism of the microlayer, an empirical correlation was proposed in terms of Reyonlds number and Weber number based on experimental data. In the region of small Weber number, linear increase of the nondimensional microlayer thickness with Weber number was concluded definitely by amount of experimental data. However, for the region in which the Weber number is bigger than 110, there is still degree of uncertainty because the data is not sufficient.

Therefore, in the present study dielectric fluid HFE-7200 was adopted as test liquid not only because its application for cooling of electronic equipment as aforementioned but also for its relative high ratio of density and surface tension which makes it possible to get data of high Weber number.

## EXPERIMENTAL APPARATUS AND PROCEDURE

A schematic diagram of the experimental apparatus is shown in Fig. 2(a). The vapor generator is located between a He-Ne laser emitter and a Pb-Se detector. A liquid reservoir and heating tank were placed upstream in the mini-gap test apparatus. The cross-section area of the liquid reservoir was large enough to maintain a constant liquid level in the mini-gap, which could ensure it was close to pool boiling in the mini-gap but not flow boiling. The liquid supplied to the mini-gap apparatus was boiled in a heating tank to exclude non-condensable and retain the temperature of liquid to be saturation. An orifice on the inlet of mini-gap was used to restrain the fluctuation of liquid flow rate caused by the bubbles growth and collapse. Vapor generated from the mini-gap vapor generator flowed through a condenser and back to the reservoir. Figure 2(b) shows the details of the mini-gap test apparatus. Quartz glass with a high transparency for infrared light was mainly utilized for the test apparatus to enable more accurate measurements. The channel thickness between two parallel quartz glass plates has a variable thickness by altering the spacers. Three different gap sizes of 0.15mm, 0.3mm and 0.5mm were adopted in this study. And the real gap size of the mini-gap, as measured with a plastic-gauge, was in the range of 0.147-0.158mm for a 0.15mm test gap size. Therefore it was confirmed that the gap size was constant and sufficiently accurate with respect to the target value as reported by Utaka et al. [1].

Passages for high temperature air used as the heating source to heat the mini-gap were positioned at the back and the front of the mini-gap. The central part of the 82mm-high passage, which essentially served as the heating area, was narrowed to enhance heating. The width of the passage was 45 mm. The heat flux into the mini-gap was controlled by varying the air temperature. A cavity of 30 μm diameter was located 12 mm below the center of the mini-gap to provide an incipient bubble site on the heating plate. The principle of the laser extinction method was used to determine the microlayer thickness by

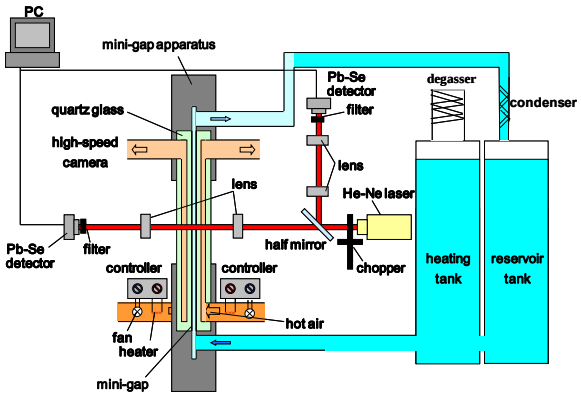


(a)Schematic of whole experimental system

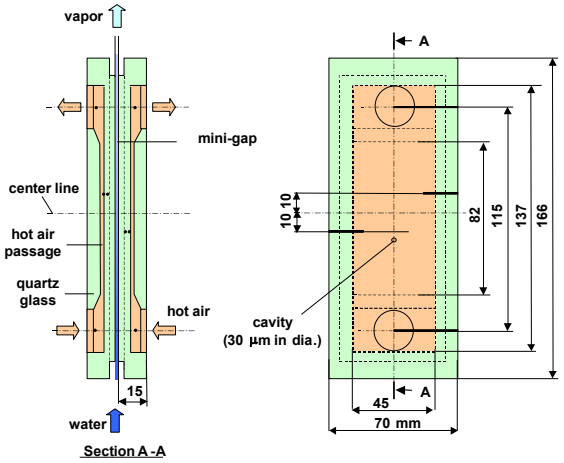


(b)Details of mini-gap and heat transfer plate

Fig. 2 Experimental apparatus for measuring microlayer thickness.

Lambert's law as shown in equation (1).

$$\delta = -(\frac{1}{A})\ln(I / I_0) \quad (1)$$

$\delta$ denotes the thickness of liquid layer the laser travels through. In this experiment, because the bubble formed symmetrically in the mini-gap, the initial microlayer thickness $\delta_0$ cited in this paper calculated as $\delta_0=0.5\delta$. Regarding to the experiment it refers to the first signal appearing on the laser ray detector when the bubble passed through the point where the laser ray passed through the minichannel, which has been reported by Utaka et al. in Ref.[1] $A$ represents the extinction coefficient, as shown in Table 1. $I_0$ denotes the light intensity at the detector when the mini-gap being measured is filled with steam and when filled with both a thin liquid layer and steam, it is denoted by $I$. This method is sufficiently accurate to measure the microlayer thickness on a micron scale, and a detailed investigation about its measurement precision has been carried out by Utaka and Nishikawa [2] for measuring the thickness of thin condensates of liquid mixtures during process of water-

Table 1 Extinction coefficient of the test fluids

| | Water | Ethanol | Toluene | HFE7200 |
|---|---|---|---|---|
| $A(\mathrm{m}^{-1})$ | $5.42\times10^4$ | $1.22\times10^5$ | $3.15\times10^4$ | $1.88\times10^4$ |

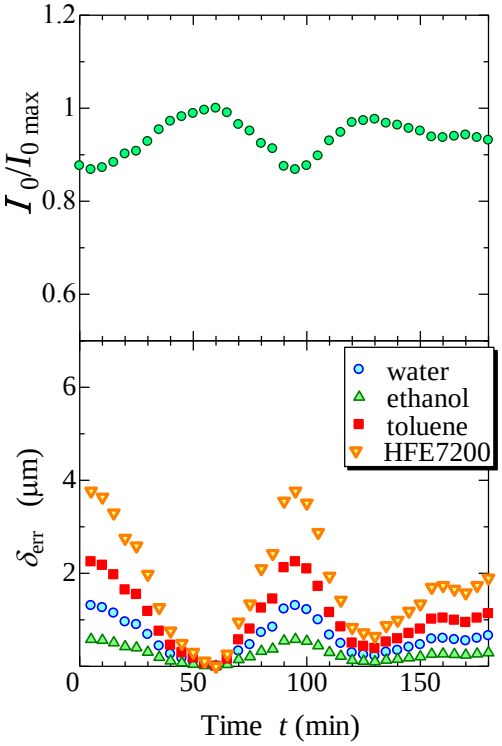


Fig.3 Error of microlayer thickness measurement due to variation of ambient temperature

-ethanol Marangoni dropwise condensation. The effects of ambient temperature change, reflection of laser rays, *etc*. on the values of $I_0/I$ were examined. As a result, it was shown that ambient temperature change was the main effect for the accuracy and the measurement error of the liquid condensates was approximately ±0.3 μm. In this study, the laser measurement devices have been improved and the accuracy of microlayer thickness measurement is different for the three kinds of testing liquid because of the difference in extinction coefficients. Figure 3 shows the variation of detector output due to ambient temperature change, where $I_{0max}$ is the max value of $I_0$ during all the test period. The largest error for microlayer thickness due to the instability of detector was 1.3μm, 0.6μm, 2.3μm and 3.9μm for water, ethanol, toluene and HFE7200 respectively. The laser signals were recorded in synchronization with the process of bubble growth, which was recorded with a high-speed camera, as shown in Fig. 2. The relative location of the incident laser ray on the heating surface was adjusted to vary the distance from the incipient bubble site.

## RESULTS AND DISCUSSION

The microlayer forms as a result of liquid remaining on the heating surface immediately after the liquid is pushed away by the bubble growth. The microlayer thickness varies due to the

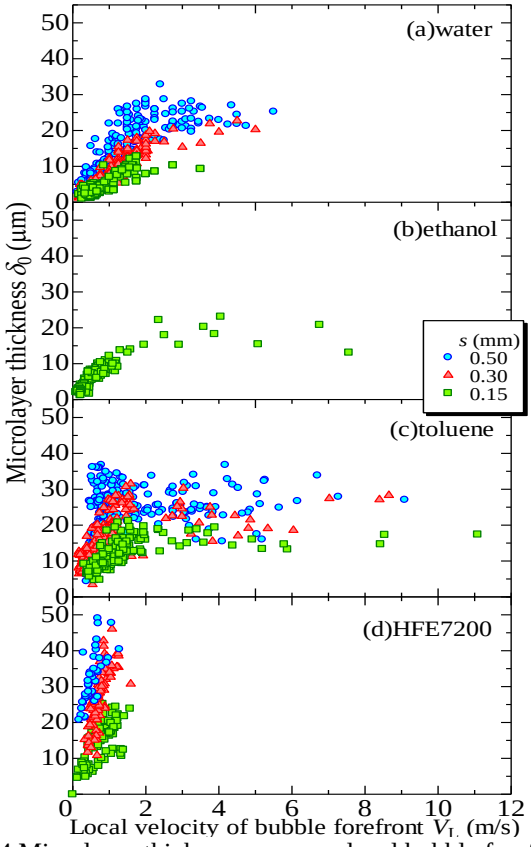


Fig. 4 Microlayer thicknesses versus local bubble forefront velocity for water, ethanol, toluene and HFE7200.

effects of bubble growth rate. In this study, attention was focused on the initial microlayer thickness $\delta_0$, which determines the basic characteristics of heat transfer in mini-gap.

The variation of the initial microlayer thickness versus the bubble forefront velocity is shown in Fig. 4 for water, ethanol, toluene and HFE7200 with three different gap sizes of 0.5, 0.3, and 0.15 mm. It was observed that the results for HFE7200 acquired until now showed a similar tendency as the other three kinds of testing fluids employed in previous report for any size of gaps, i.e. at low velocity regions, the microlayer thickness increases almost linearly with forefront velocity. This is because in this region, the thickness of microlayer is determined by a balance between the viscous force (which is favorable to the microlayer increasing by leaving the liquid adhesion to the wall) and the capillary force (which trend to limit the microlayer). Thus, as the forefront velocity become fast, the viscous force increased due to the gradient of velocity near the wall become bigger. Moreover, the initial microlayer thickness was strongly affected by the gap size, and it decreased with decreasing gap size. The qualitative explanation was considered as following: the pressure within the bubble may be regarded as approximately uniform, then according to the Yong-Laplace equation for the interface pressure difference the surface tension products pressure drop within liquid between flat microlayer region and tip region due to the

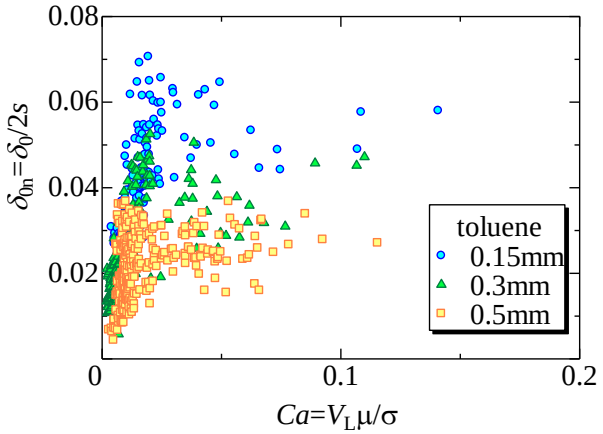


Fig.5 Nondimensional microlayer thickness versus capillary number for toluene.

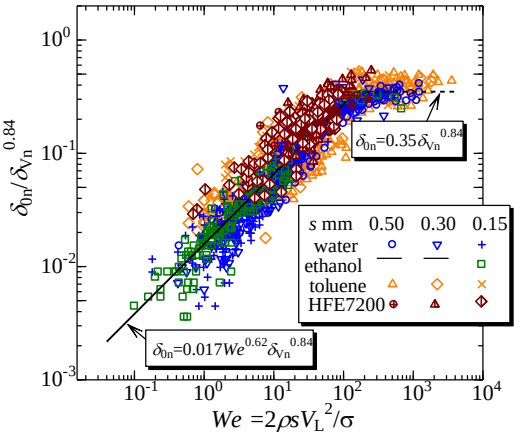


Fig.6 Dependence of the initial microlayer thickness on the Weber number and the viscous boundary layer thickness

different curvature of interface that is almost zero for the flat microlayer region and probably 2/*s* for the tip as shown in Fig.1. Therefore, as gap size decreasing the bubble inside the channel was confined greater and the curvature of the tip increases while the curvature of flat microlayer region is still probably zero without any change, correspondingly pressure drop between the two region aforementioned become greater and much more amount of liquid was pushed out from the microlayer to the tip region by the surface tension, which makes the microlayer thinner.

Since the viscous and capillary forces play antagonist roles, the natural correlation form for the experiment results is proposed as equation (2) by several researchers [3-6] for the capillary tube and adiabatic condition, where $Ca=\mu V_L/\sigma$ is the capillary number, $\mu$ being the liquid viscosity and $V_L$ the bubble forefront velocity.

$$\delta_{0n} = \frac{\delta_0}{2s} = \varphi(Ca) \qquad (2)$$

As to this research, the normalized microlayer thickness based on gap size was plotted versus *Ca* as Fig.5 for the results of toluene which has most sufficient data in wide range of bubble forefront velocity among the four kinds of liquids used in this paper until now. It can be found that the results in the region of low velocity are correlated well by *Ca* without difference in the effect of gap size. But obvious definite relation cannot be observed in the region of high velocity, i.e. microlayer thickness normalized by the gap size distributes in the opposite order versus the gap size. The two contrary tendency makes it clear that for one kind of liquid the microlayer thickness is determined to be a definite fraction of gap size in the low velocity region (because the bubble is almost confined proportional with the gap size), but not in the high velocity region. In the latter region, the effect of inertia is considered to become non-ignorable factor, and correspondingly the microlayer in this region becomes to show the feature of boundary layer for the case of flow in the inlet length of a straight gap. Near in the inlet section the boundary layer develops in the same way as on a flat plate, therefore the

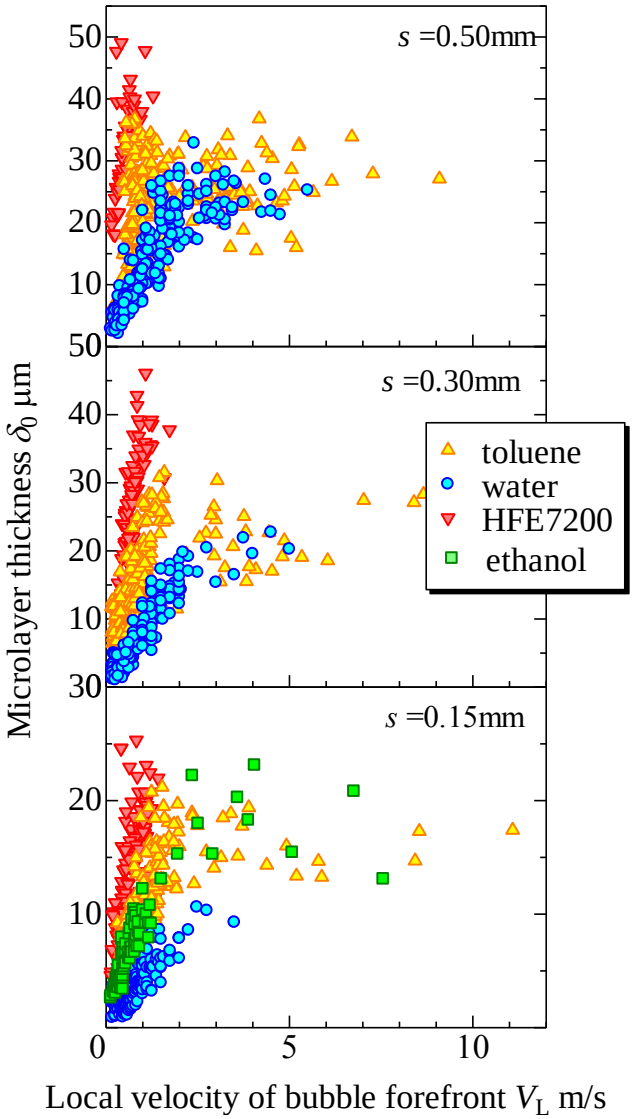


Fig. 7 Effect of fluid properties on initial microlayer thickness for s=0.5, 0.3 and 0.15 mm.

thickness of boundary layer does not increase proportional with the gap size which is quite different with the microlayer determined by viscous and capillary force.

In order to make a comprehension for the both velocity regions, a simple inquiry will be attempted in another way as following. Inside the mini-gap after growing to almost the size of gap, the bubble grows mainly in the direction that parallel to the wall of gap. At the same time, the liquid ahead of the bubble is pushed away and begin to flow similar as the flow in the inlet length of channel, and boundary layer is formed on both sides of walls. According to Prandtl law, for the case of low velocity the boundary layer formed near the walls is very thick comparing to the thickness of microlayer formed by the balance of viscous and capillary forces. Then with the growing of bubble, top part of boundary layer is push away by the bubble. Therefore it is considered that the microlayer thickness as being limited by both the surface tension effect due to the gap size and boundary layer formation. And with the velocity increasing, the effect of boundary layer becomes more and more important for the thickness of boundary layer decreases and approaches to the same magnitude as the microlayer thickness determined by surface tension and viscous force. Therefore, the contrary tendency between the results shown in Fig.4(c) and Fig.5 at the high velocity region maybe make sense with the fact that the microlayer in this region has both the feature of boundary layer and viscous-capillary determined microlayer.

In order to get a proper correlation for the experimental data and gain general insight into the controlling mechanism without considering the kind of fluid and operating conditions, the dimensionless parameters $Re=\rho V_L d_h/\mu$ and $We=\rho V_L^2 d_h/\sigma$ (based on hydrodynamic diameter $d_h=2s$) were used to analyze the experimental results in the previous report [1]. It was found that the normalized microlayer thickness based on Prandtl law increased as a function of Weber number as equation (3) at the region where $We<110$.

$$\delta_{0n} = 0.017We^{0.62}\delta_{Vn}{}^{0.84}$$

$$= 0.017We^{0.62}\left(\frac{D}{2s}\right)^{0.42}(Re)^{-0.42} \quad (3)$$

After adding the data of HFE7200, the results are displayed in Fig.6 where $\delta_{0n}$ is nondimensional microlayer thickness as shown in equation (4) and $\delta_{Vn}$ is the nondimensional boundary layer defined as equation (5).

$$\delta_{0n} = \delta_0/2s \quad (4)$$

$$\delta_{Vn} = \frac{\delta_V}{2s} = \frac{1}{2s}\sqrt{\frac{\mu D}{\rho V_L}} = \sqrt{\frac{D}{2s}}\cdot\frac{1}{\sqrt{Re}} \quad (5)$$

It can be observed that empirical correlation obtained by least squares fitting with the experimental data of water, ethanol and toluene in previous report is still fit well with the result of HFE7200 at the region of small *We*. According to equation(3) and the definition of Weber number, at the region of small velocity the thickness is proportional to $\rho^{0.62}\nu^{0.42}\sigma^{-0.62}$ and it is 1.75,1.40 ,0.74 and 2.61for ethanol, toluene, water and HFE7200 respectively according to their properties as shown in Table 2. A finding also was supported by the experimental results. Figure 7 shows the effect of fluid properties on initial microlayer thickness for $s$ = 0.5, 0.3 and 0.15 mm. As shown in Fig. 7(c), for toluene and ethanol, whose value of $\rho^{0.62}\nu^{0.42}\sigma^{-0.62}$ are close to each other, their thicknesses are approximate in the region of relatively lower velocity. In the same way, because the value of $\rho^{0.62}\nu^{0.42}\sigma^{-0.62}$ for water and HFE7200 are smallest and biggest values, respectively, the microlayer thickness of water and HFE7200 are the thinnest and thickest respectively in all the four kinds of testing liquid. Similar as the explanation of gap size effect for Fig.4, that the greater flow of liquid from flat microlayer region to tip region could be caused by the fluid with bigger surface tension when the gap size and velocity is the same.

It shows that further studies are required of transient microlayer formation with the accelerating growth of bubble confined in mini-gap over the range of conditions relevant to boiling at region of large velocity, where the effect of surface tension should not be omitted completely but to be reconsidered.

## CONCLUSIONS

Experiments were performed to directly measure, by the laser extinction method, the microlayer that forms on a heating surface by vapor growth during boiling in mini-gap that formed by two parallel quartz glass for the liquid of HFE7200. Microlayer thickness became smaller as the gap size decreases regardless testing liquid type. The microlayer for HFE7200 is the thickest during all the test liquids. A dimensionless correlation for investigating the effects of test liquids and gap sizes on microlayer thickness presented in previous report was found to be applicative for the dielectric fluid HFE-7200 at small Weber number (*We*<110). In this region the microlayer is controlled mainly by Weber number, its thickness being thinner for the liquid whose value of $\rho^{0.62}\nu^{0.42}\sigma^{-0.62}$ was relatively small comparing with other testing liquid. And region of big *We* region i.e. bubble grows with high forefront velocity was remained to be studied in the future research.

## NOMENCLATURE

| | |
|---|---|
| $A$ | extinction coefficient ($m^{-1}$) |
| $d_h$ | hydraulic diameter |
| $D$ | distance from incipient bubble site (mm) |
| $I$ | laser intensity |
| $I_0$ | incident laser intensity |
| $s$ | gap size (mm) |
| $d_h$ | hydrodynamic diameter(mm) |
| $V_L$ | local bubble forefront velocity (m/s) |
| $\delta$ | thickness of liquid layer the laser travels through (μm) |
| $\delta_0$ | initial thickness of microlayer (μm) |

$\delta_{0n}$ nondimensional initial thickness of microlayer
$\delta_{Vn}$ nondimensional viscous boundary thickness
$\nu$ kinematic viscosity ($mm^2/s$)
$\mu$ viscosity(μPa・s)
$\sigma$ surface tension coefficient (mN/m)
*We* Weber number
*Re* Reynolds number
*Ca* Capillary number

## ACKNOWLEDGMENTS

This work was supported in part by a Grant-in-Aid for Scientific Research of the Ministry of Education, Culture, Sports, Science and Technology, Japan [(B) 17360096].

## REFERENCES

[1] Yaohua Zhang,Utaka,Y.,Kashiwabara Y.,and Kamiaka T.2009,Characteristics of Microlayer Thickness Formed During Boiling in Microgaps,ICNMM2009-82244
[2] Utaka, Y. and Nishikawa, T., 2003,An investigation of liquid film thickness during Solutal Marangoni condensation using laser absorption method: absorption property and examination of measuring method, *Heat Transfer-Asian Res*.**30** (8), pp. 700-711.
[3] Taylor, G.I., 1961, Deposition of a viscous fluid on the wall of a tube, *J. Fluid Mech*., **10**, pp. 1161-1165.
[4] Bretherton, F.P., 1961, The motion of long bubbles in tubes, *J. Fluid Mech*. **10**, pp. 166-188.
[5] Katto, Y. and Yokoya. S, 1966, Experimental study of nucleate pool boiling in case of making interference plate approach to the heating surface, *Proc. 3rd Int. Heat Transfer Conf*., 3, pp. 219-227.
[6]Katto,Y.,and Shoji,M., 1970, Principal Mechanism of Micro-Liquid-Layer Formation on a Solid Surface With a Growing Bubble in Nucleate Boiling. *Int.J.Heat Mass Transfer* ,.Vol.13,p.1299